Electronic Supplementary Information

Two dimensional hierarchical architectures fabricated by the self-assembly of Poly(3-hexylthiophene)-*b*-Polyethylene Glycol

Rui Qi,[a] *Yulin Zhu,*[b] *Liang Han,*[b,c] *Meijing Wang,*[b] *and Feng He**[b,c]

[a] · College of Food and Biological Engineering, Chengdu University, Chengdu 610106, P. R. China

[b] · Shenzhen Grubbs of Institute and Department of Chemistry, Southern University of Science and Technology, Shenzhen, 518055, China. Email: hef@sustech.edu.cn

[c.] Guangdong Provincial Key Laboratory of Catalysis, Southern University of Science and Technology, Shenzhen, 518055, China.

Contents

1.Materials

2, 5-dibromo-3-hexylthiophene, tertbutyl-magnesium chloride (1.0Min THF), 6-azidohexanoic Acid, copper (I) bromide, sodium azide, ethynylmagnesium chloride (0.5 M in THF), [(1,3-diphenylphosphino)-propane]-dichloronickel [Ni(dppp)Cl2] and pentamethyldiethylenetriamine (PMDETA) were purchased from Sigma-Aldrich and used without further purification. Methoxypolyethylene glycol (PEG, M_n = 550 $g \cdot mol^{-1}$) was purchased from Aladdin and used as received. Tetrahydrofuran (THF) and dichloromethane (DCM) were purified before use with double alumina and alumina/copper catalyst drying columns from Anhydrous Engineering Inc. Oxalyl chlorazide, $Na_2S_2O_3$, anhydrous $MgSO_4$, anhydrous Na_2SO_4, dimethylformamide (DMF, AR), hexane (AR), acetonitrile (AR), ethyl acetate (AR), methanol (HPLC), ethanol (HPLC), isopropanol (*i*-PrOH, HPLC) and isobutanol (HPLC) were purchased from J&K Scientific Ltd. and used without further purification.

2. Synthesis of the di-block copolymer

2.1 Synthesis and Characterization of Ethynyl-P3HT$_{10}$

Ethynyl-P3HT$_{10}$ was synthesized according to our previous reported,[1] as shown in Scheme S1. The whole synthesis process was carried out in a glovebox under an argon atmosphere, as follows. In a flame-dried 100 mL one-neck round-bottom flask, 5.0 g (15.3 mmol) of 2, 5-dibromo-3-hexylthiophene dissolved in freshly distilled dry THF (37 mL) was stirred for 30 min at room temperature. After injecting 15.3 mL of tert-butyl-magnesium chloride (1.0 M in THF) to the flask, the mixture solution was stirred at room temperature overnight to complete the metal-halogen exchange reaction. 320.0 mg (0.59 mmol) of Ni(dppp)Cl_2 and 145 mL of THF were added to a 250 mL one-neck round-bottom flask. After being stirred for 2 h at 40 °C, the mixture solution in 250 mL flask was cooled to 30 °C. Then, the activated Grignard monomer solution in 100 mL flask was transferred into the 250 mL flask by a syringe and stirred for 30 min at 30 °C. The termination reaction and functionalization were carried out by the one-shot addition of ethynylmagnesium bromide (9.0 mL, 0.5 M in THF). The mixture was stirred for 10 min and then poured into cold methanol for quenching. The precipitate was extracted

by the soxhlet method using, successively, methanol and acetone. The desired ethynyl-P3HT (480 mg, yield=9.6%) was obtained by extraction with acetone and dried under reduced pressure. The degree of polymerization was estimated to be 10 from the ^{1}H NMR spectrum (Fig. S1). GPC (Fig. S6): $\boldsymbol{M}_n$ = 1734 g·mol^{-1}, PDI = 1.07. MALDI-TOF MS (Fig. S2): m/z = 1582 (calcd), PDI = 1.02. ^{1}H NMR (400 MHz, $CDCl_3$): δ (ppm) = 6.97 (s, 1H), 3.52 (s, 1H), 2.78 (t, 2H), 1.68 (t, 2H), 1.34-1.42 (m, 6H), and 0.90 (t, 3H).

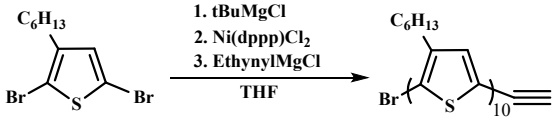

Scheme S1 Synthesis of $P3HT_{10}$.

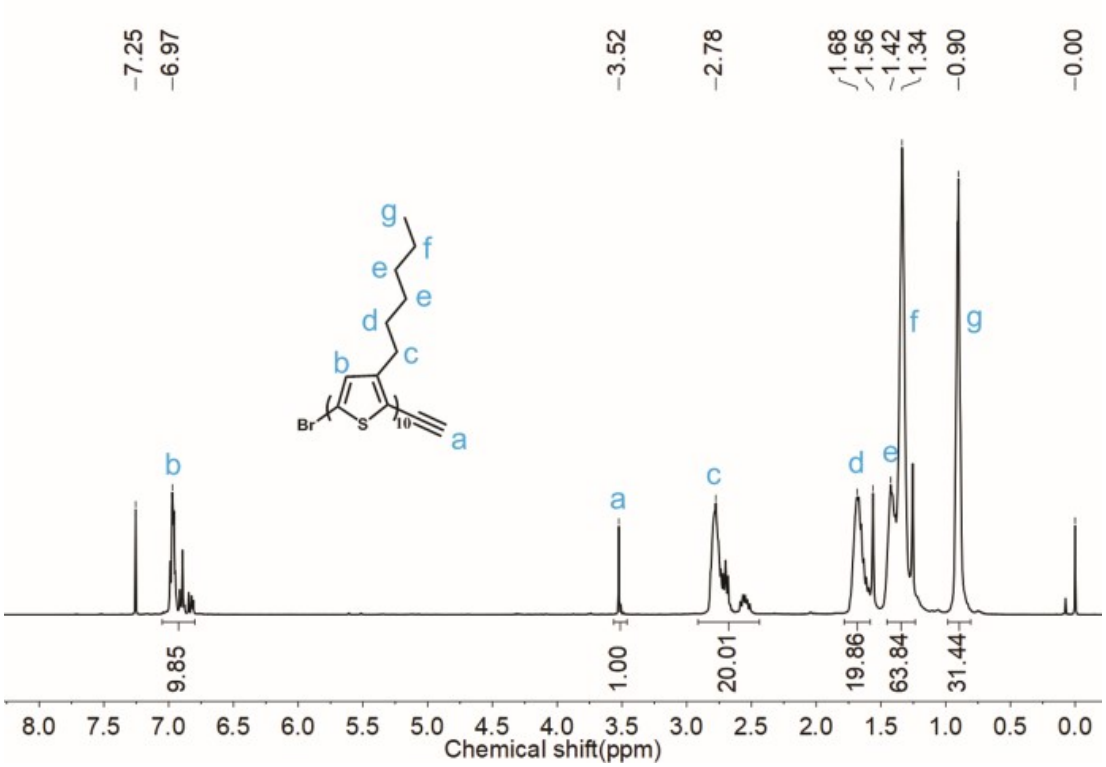

Fig. S1 ^{1}H-NMR spectrum of $P3HT_{10}$.

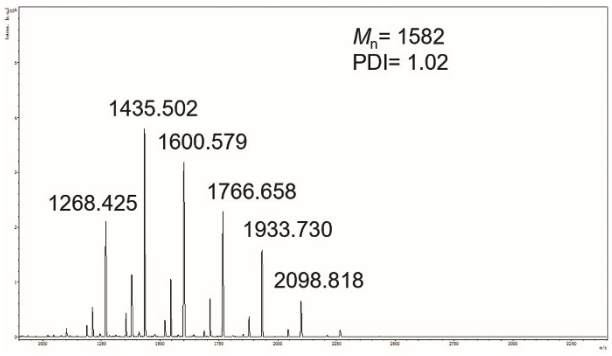

Fig. S2 MALDI-TOF mass spectra of $P3HT_{10}$. The repeat unit was 166.08 m/z.

2.2. Synthesis and Characterization of PEG_{12}-N_3

The synthesis of PEG_{12}-N_3 was shown in Scheme S2. In a flame-dried 150 mL one-neck round-bottom flask, 678.0 mg (4.3 mmol) of 6-azidohexanoic acid dissolved in DCM (15 mL) and 1 mL (11.82 mmol) of oxalyl chlorazide were mixed at room temperature. After stirring for 12 h under an argon atmosphere at room temperature, the solvent and the residual oxalyl chlorazide were evaporated under vacuum. Then, 3 mmol of PEG_{12} dissolved in DCM (15 mL) was added to the flask under an argon atmosphere. After cooling to 0 °C, 0.91 g (9 mmol) of anhydrous triethylamine was added dropwise. The mixture solution was stirred overnight at room temperature. The solvent was evaporated under vacuum, and then 30 mL of ethyl acetate was added. After washing with deionized water (3 × 50 mL), the organic layer was dried over anhydrous Na_2SO_4 and the ethyl acetate was evaporated under vacuum. The unreacted 6-azidohexanoic acid was removed by column chromatography using hexane/ethyl acetate (4:6) as the eluent, while the desired product was obtained through column chromatography using ethyl acetate/methanol (20:3) as the eluent. Drying under high vacuum at room temperature afforded the desired product. Characterization of PEG_{10}-N_3 (1.62 g, yield=78.3%): the purity was estimated to be 50% by the ^{1}H NMR spectrum (Fig. S4). ^{1}H NMR (400 MHz, $CDCl_3$): δ (ppm) = 3.65 (m, 4H), 3.38 (s, 3H), 3.28 (t, 2H), 2.36 (t, 2H), 1.65 (m, 4H), and 1.41 (m, 2H). FT-IR (cm^{-1}) (Fig. S3): 2098.5 (azide).

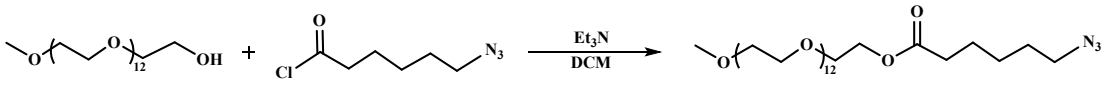

Scheme S2 Synthesis of PEG_{12}-N_3.

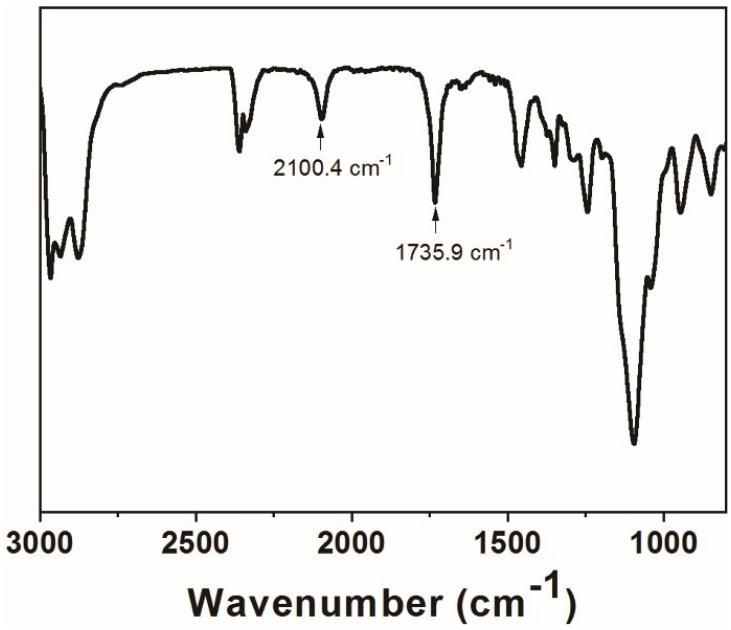

Fig. S3 FT-IR spectrum of PEG_{12}-N_3.

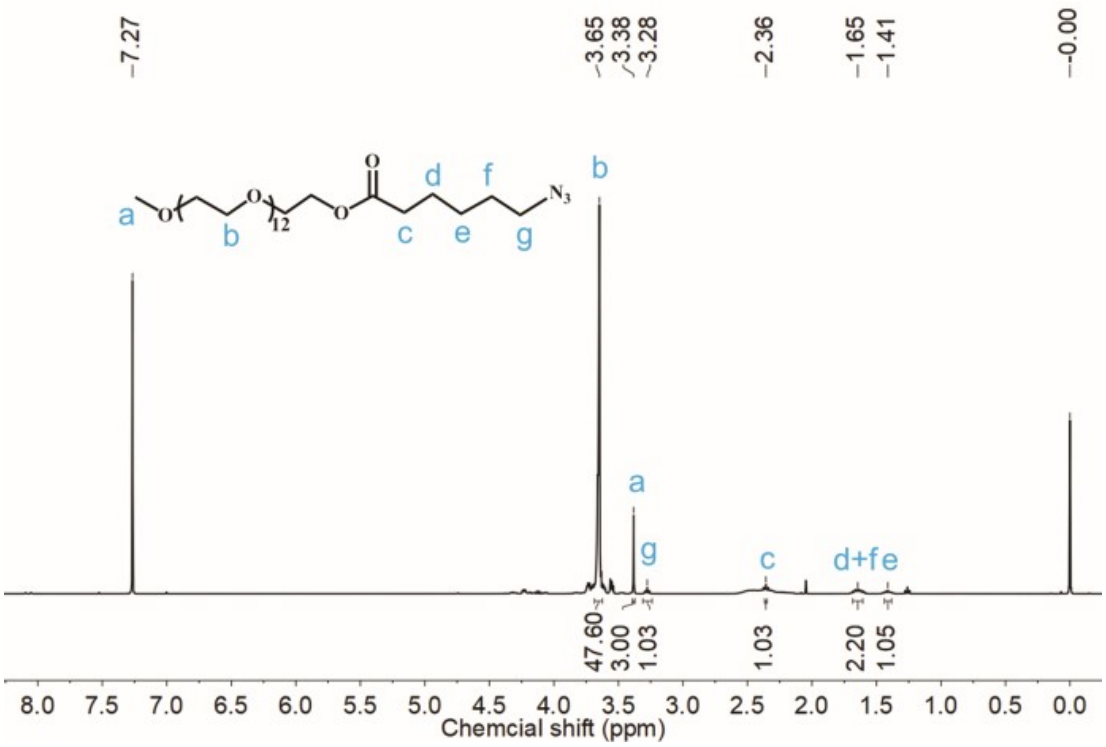

Fig. S4 ^{1}H-NMR spectrum of PEG_{12}-N_3.

2.3 Synthesis and Characterization of $P3HT_{10}$-*b*-PEG_{12}

The synthesis of $P3HT_{10}$-*b*-PEG_{12} was shown in Scheme S3. Ethynyl-$P3HT_{10}$ (0.12 mmol), PEG_{12}-N_3 (0.30 mmol), and PMDETA (1.0 μL, 0.50 mmol) in freshly distilled dry THF (30 mL) were added to a one-neck round-bottom flask (100 mL) equipped with a magnetic stir bar and an argon-vacuum inlet/outlet. After three cycles of freeze-pump-thaw, the mixture was transferred into a glovebox under an argon atmosphere. CuBr (1.0 g, 0.50 mmol) was then added into the flask. The reaction mixture was stirred for 4 days at 40 °C. Cu/PMDETA was removed by passing the solution through an alumina column with THF as the eluent. The unreacted P3HT and unreacted PEG were removed by silica column chromatography using chloroform and chloroform/methanol (1:2) as the eluent, respectively. The desired product (152 mg, yield=52.3%) was obtained through column chromatography using chloroform/methanol (10:1) as the eluent. For $P3HT_{10}$-*b*-PEG_{12}, GPC (Fig. S6): $\boldsymbol{M}_n$ =3020 g·mol^{-1}, PDI = 1.08, and the block ratio of P3HT/PEG was estimated to be 1:1 by the ^{1}H NMR spectrum (Fig. S5). ^{1}H NMR (400 MHz, $CDCl_3$): δ (ppm) = 6.97 (s, 1H), 3.68 (m, 4H), 3.37 (s, 3H), 3.28 (t, 2H), 2.80 (t, 2H), 2.36 (t, 2H), 1.71 (t, 2H), 1.63 (m, 4H), 1.33-1.42 (m, 8H), and 0.89 (t, 3H).

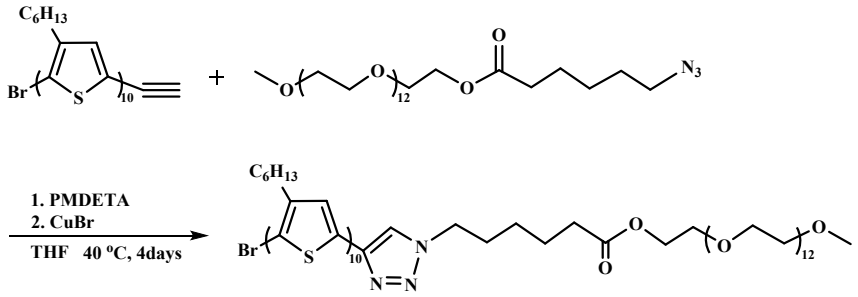

Scheme S3 Synthesis of $P3HT_{10}$-*b*-PEG_{12}.

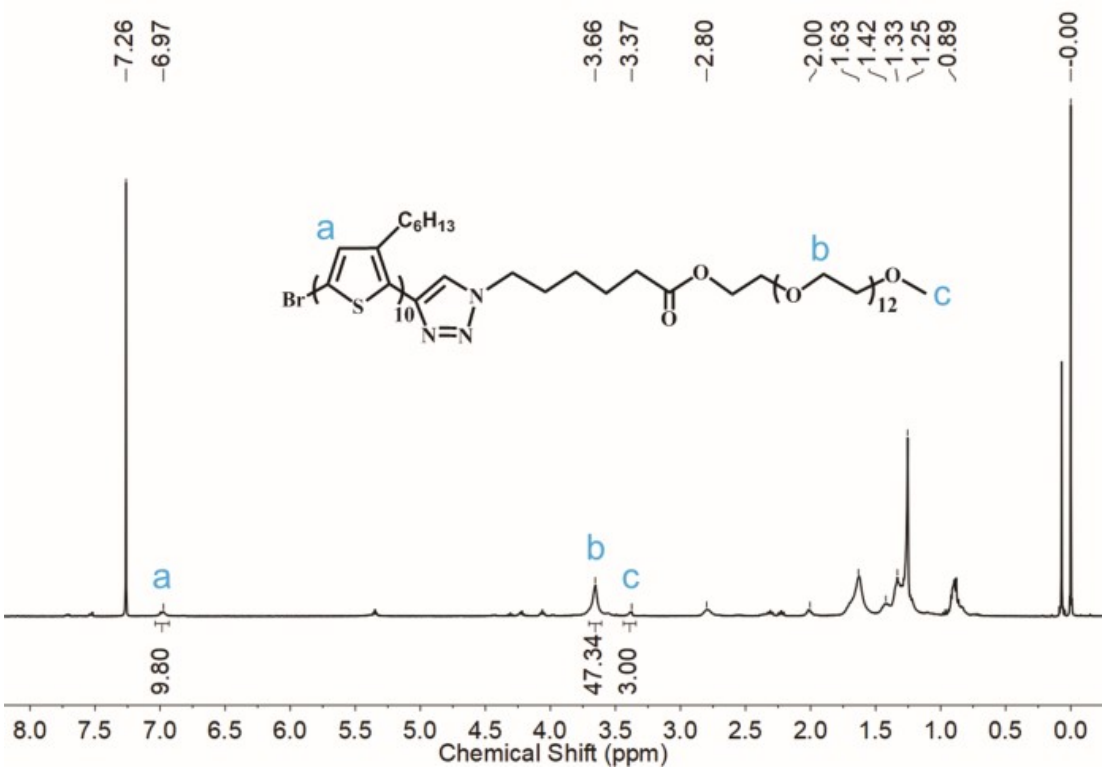

Fig. S5 ^{1}H-NMR spectrum of P3HT$_{10}$-*b*-PEG$_{12}$.

3. Preparation of polymer micelles

The stoichiometric P3HT$_{10}$-*b*-PEG$_{12}$ in THF (0.5 mg mL^{-1}) was first added to a 20 mL sealed vial. After solvent evaporation at rt (25 °C), 60 μL of THF was added to dissolve the polymer. Then, 6 mL of solvent was added dropwise to the vial with magnetic stirring. After treatment with ultrasonic waves for 30 min, the solutions were heated at a fixed temperature (*i*-PrOH 80°C, isobutanol 80°C, CH_3CH_2OH 75°C, CH_3OH 65°C) for 2 h and then slowly cooled down to rt (25 °C), followed by aging for 12 h at 25 °C. The obtained micelles were used for the respective experiments.

4. Polymer Characterization

^{1}H nuclear magnetic resonance (^{1}H NMR). The ^{1}H NMR spectra were measured on a Bruker AVANCE 400 MHz spectrometer with $CDCl_3$ as the solvent.

Fourier transform infrared spectrometer (FT-IR). Fourier transform infrared spectra (FT-IR) were obtained on a Perkin-Elmer system 2000 FT-IR spectrometer.

Gel permeation chromatography (GPC). GPC measurements were carried out on a Viscotek VE 2001 triple-detector gel permeation chromatograph equipped with an automatic sampler, a pump, an injector, an inline degasser, and a column oven at 40 °C. THF was used as the eluent, with a flow rate of 1.0 mL min^{-1}. Samples were dissolved in the eluent (1 mg mL^{-1}) and filtered with an organic-phase filter (polytetrafluoroethylene membrane with 0.45 mm pore size) before analysis. The calibration was conducted using a PolyCALTM polystyrene standard from Viscotek.

Matrix-assisted laser desorption ionization time-of-flight mass spectrometry (MALDI-TOF MS). MALDI-TOF MS spectra were recorded on a Bruker Flex Series MALDI-TOF MS in positive-ion reflectron mode with an accelerating voltage of 20 kV. The samples were prepared by mixing a THF solution of 2,2′:5,2″-terthiophene matrix solution (0.25 M) and a THF solution of P3HT (10 $mg \cdot mL^{-1}$**).**

Transmission Electron Microscopy (TEM). 10 μl of the polymer solutions were quickly obtained from the solutions at different temperatures using a 100 microliter pipette, and then were drop-casted onto the carbon-coated copper grids as soon as possible. The samples were prepared after evaporating the solvents at the room temperature. TEM images were obtained on a Hitachi HT7700 microscope operating at 100 kV and equipped with an AMF-5016 charge-coupled device camera.

Helium ion microscope (HIM). The samples were prepared by putting a drop of solution of assemblies on carbon-coated copper grids followed by solvent evaporated. The grids were put on conducting resin for observation. The characterization was carried by a Carl Zeiss, ORION NanoFab helium ion microscope under conditions:

30KeV Acc. voltage, ~0.7 pA beam current, 2 μs dwell time, 2.6E-6 Millibar GFIS gun pressures, 7.7 mm working distance and line scan mode.

Atomic Force Microscopy (AFM). The AFM samples were prepared by drop casting 10 μl of the polymer solutions onto the carbon-coated copper grids, and then evaporating solvents. Imaging was performed on an Asylum Research AFM in AC mode under ambient conditions. The silicon probe reflex coated with aluminum manufactured by Budget sensor Company was used as the sensor cantilevers. Images were obtained by IGOR Pro software (WaveMetrics Inc).

Grazing Incidence Wide-angle X-ray Scattering (GIWAXS). The sample was prepared by drop-coating 60 μl of the micelle solution onto the pre-cleaned and treated silicon wafer followed by evaporating the solvent for seven times. The silicon wafer was cleaned in piranha solution for 30 min, then ultrasound successively in ethanol, ultrapure water, and finally dried with blowing nitrogen. GIWAXS measurement was performed at the 8ID-E beamline at the Advanced Photon Source, Argonne National Laboratory, using X-rays with a wavelength of λ =1.1385 Å, and a beam size of 200 μm (h) and 20 μm (v). A 2-D PILATUS 1M-Fdetector was used to capture the scattering patterns and was situated at 208.7 mm from sample. Typical GIWAXS pattern was taken at an incidence angle of 0.13°, above the critical angles of conjugated polymer and below the critical angle of the silicon substrate. Consequently, the entire structure could be detected. In addition, the q_y scan was obtained from a linecut across the reflection beam center, while the q_z scan was achieved by a linecut at $q_y = 0$ Å^{-1}, using the reflected beam center as 0.

UV-Vis Absorption Spectra (UV-Vis). The UV-Vis absorption spectra were recorded by a SHIMADZU UV3600 spectrophotometer. A sealed quartz glass cuvette filled with *i*-PrOH solution of P3HT$_{10}$-*b*-PEG$_{12}$ was placed in the holder of spectrophotometer,

which was linked with a temperature controller. The solution in cuvette was kept for 2 h at 80 °C and then spontaneous cooled to room temperature. The UV-Vis spectra and the real-time temperatures of the solutions were recorded every 15 min during the cooling process. After the solutions were cooled to room temperature, the spectra were recorded every 1 h until after aging for 12 h. The other sample solutions were tested at room temperature.

Fluorescence spectroscopy (PL spectra). The PL spectra was carried out with an Edinburgh FS5 spectrofluorometer (Edinburgh Instruments Ltd., UK). The fluorescence quantum efficiencies in *i*-PrOH were determined at a excitation wavelength (440 nm)，using Coumarin 153 as reference. A sealed quartz glass cuvette filled with *i*-PrOH solution of $P3HT_{10}$-*b*-PEG_{12} was placed in the holder of spectrophotometer, which was linked with a temperature controller. The solution in cuvette was kept for 2 h at 80 °C and then spontaneous cooled to room temperature. The PL spectra and the real-time temperatures of the solutions were recorded every 15 min during the cooling process. After the solutions were cooled to room temperature, the spectra were recorded every 1h until after aging for 12h. The other sample solutions were tested at room temperature.

5. The statistical sizes of the nanostructures

The sizes of each sample were obtained by analyzing two hundred micelles from TEM images using Digital Micrograph software (US Gatan company). The diagonal length was used to characterize the scale of the single and hierarchical 2D rectangular micelles. The diameter was used to characterize the scale of the ball-like micelles and flower-like aggregates. The length and width were used to characterize the scale of the ribbon-like micelles. The number-average diagonal length ($\boldsymbol{S}_n$) and the weight-average diagonal length ($\boldsymbol{S}_w$), the number-average diameter length ($\boldsymbol{D}_n$) and the weight-average

diameter length ($\boldsymbol{D}_w$), the number-average length ($\boldsymbol{L}_n$), the weight-average length ($\boldsymbol{L}_w$), the number-average width ($\boldsymbol{W}_n$), the weight-average width ($\boldsymbol{W}_w$) of the assemblies were calculated by the following equations: (where $\boldsymbol{S}_i$, $\boldsymbol{D}_i$, $\boldsymbol{L}_i$ and $\boldsymbol{W}_i$ are the sizes of individual micelle, respectively, $\boldsymbol{N}_i$ are the number of $\boldsymbol{S}_i$, $\boldsymbol{D}_i$, $\boldsymbol{L}_i$ and $\boldsymbol{W}_i$).

$$S_n = \frac{\sum_{i=1}^{N} N_i S_i}{\sum_{i=1}^{N} N_i}$$

$$S_w = \frac{\sum_{i=1}^{N} N_i {S_i}^2}{\sum_{i=1}^{N} N_i S_i}$$

$$D_n = \frac{\sum_{i=1}^{N} N_i D_i}{\sum_{i=1}^{N} N_i}$$

$$D_w = \frac{\sum_{i=1}^{N} N_i {D_i}^2}{\sum_{i=1}^{N} N_i D_i}$$

$$L_n = \frac{\sum_{i=1}^{N} N_i L_i}{\sum_{i=1}^{N} N_i}$$

$$L_w = \frac{\sum_{i=1}^{N} N_i {L_i}^2}{\sum_{i=1}^{N} N_i L_i}$$

$$W_n = \frac{\sum_{i=1}^{N} N_i W_i}{\sum_{i=1}^{N} N_i}$$

$$W_w = \frac{\sum_{i=1}^{N} N_i W_i^{\,2}}{\sum_{i=1}^{N} N_i W_i}$$

Table S1 The statistical sizes of the nanostructures.

Solvent	c (mg mL^{-1})	D_n (nm)	D_w (nm)	D_w/D_n	
i-PrOH[a]	0.001	2460	2779	1.13	2D micelles
i-PrOH[a]	0.005	2971	3100	1.04	2D hierarchical micelles
i-PrOH[a]	0.015	4148	4282	1.03	2D hierarchical micelles
i-PrOH[a]	0.05	6463	7658	1.18	2D hierarchical micelles
CH_3OH[b]	0.001	870	963	1.11	ball-like micelles
CH_3OH[b]	0.005	1612	1711	1.06	ball-like micelles
CH_3OH[b]	0.015	2397	2568	1.07	ball-like micelles
CH_3CH_2OH[a]	0.001	438	485	1.11	2D micelles
CH_3CH_2OH[b]	0.001	1777	1965	1.11	flower-like micelles
CH_3CH_2OH[a]	0.005	543	579	1.07	2D micelles
CH_3CH_2OH[b]	0.005	2023	2124	1.05	flower-like micelles
CH_3CH_2OH[a]	0.05	633	694	1.10	2D micelles
CH_3CH_2OH[b]	0.05	2037	2125	1.04	flower-like micelles
isobutanol[c]	0.005	85	93	1.10	nanoribbons
isobutanol[d]	0.005	3735	5517	1.48	nanoribbons

[a] represents the diagonal length (***S***) of the 2D micelles and 2D hierarchical micelles, [b] represents the diameter length (***D***) of the ball-like micelles and flower-like micelles, [c] represents the width (***W***) of the ribbon-like micelles, [d] represents the length (***L***) of the ribbon-like micelles.

6. GPC trace (UV-Vis) of the homopolymer and diblock copolymer.

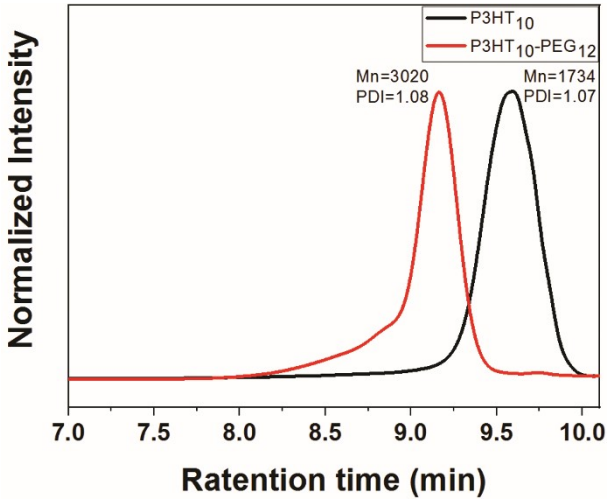

Fig. S6 GPC trace (UV-Vis) of $P3HT_{10}$ and $P3HT_{10}$-*b*-PEG_{12} in THF.

7. The TEM images of the nanostructures formed by $P3HT_{10}$-*b*-PEG_{12} in *i*-PrOH using different polymer concentrations.

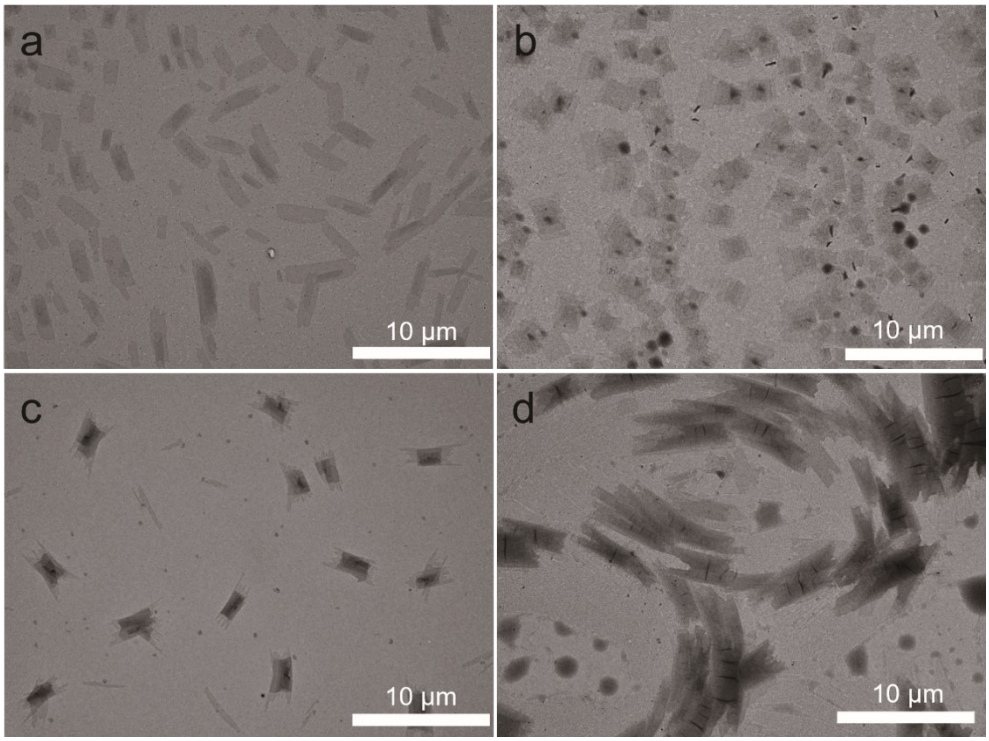

Fig. S7 TEM images of 2D nanostructures formed by $P3HT_{10}$-*b*-PEG_{12} in *i*-PrOH using different polymer concentrations, a) 0.001 mg mL^{-1}, b) 0.005 mg mL^{-1}, c) 0.015 mg mL^{-1}, d) 0.05 mg mL^{-1}.

8. The size distributions of the nanostructures formed by P3HT$_{10}$-*b*-PEG$_{12}$ in *i*-PrOH using different polymer concentrations.

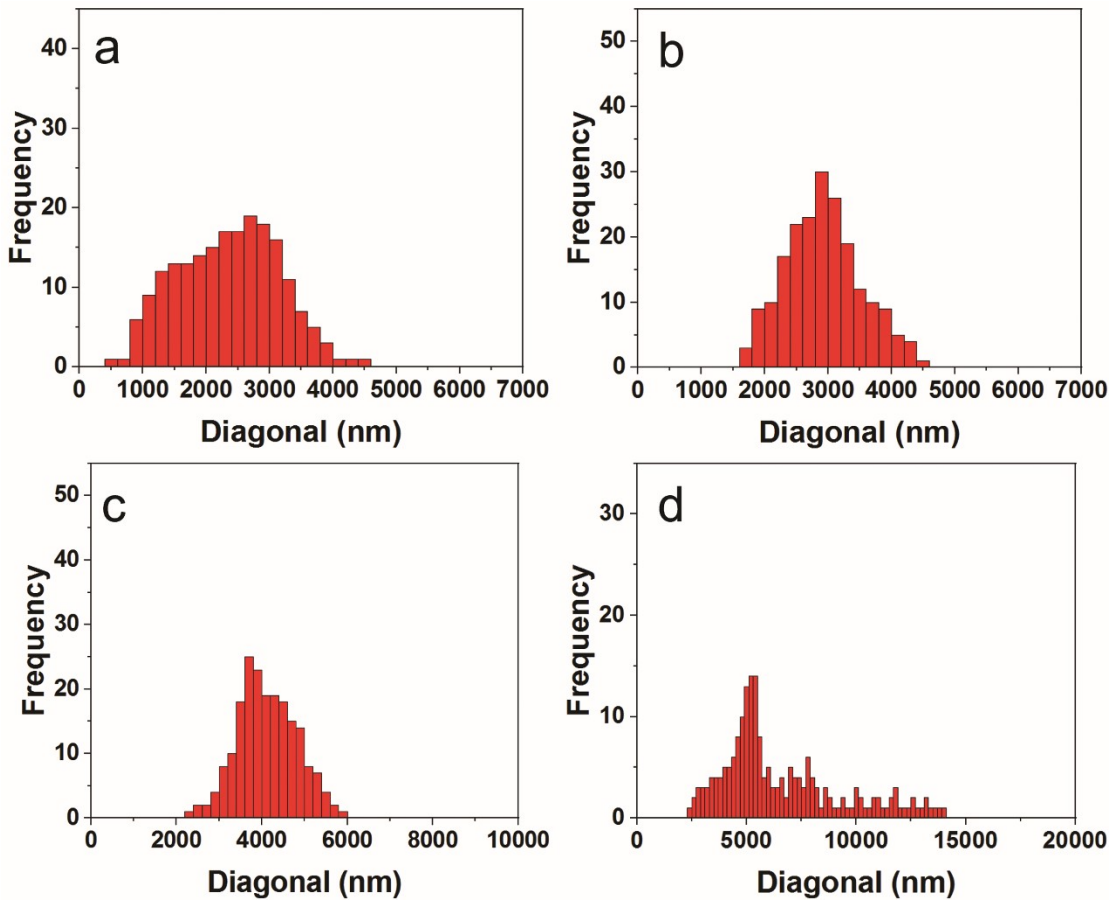

Fig. S8 The contour length distributions of the diagonal length of correspondent 2D nanostructures formed by P3HT$_{10}$-*b*-PEG$_{12}$ in *i*-PrOH using different polymer concentrations, a) 0.001 mg mL^{-1}, b) 0.005 mg mL^{-1}, c) 0.015 mg mL^{-1}, d) 0.05 mg mL^{-1}.

9. The AFM images of the nanostructures formed by P3HT$_{10}$-*b*-PEG$_{12}$ in *i*-PrOH using different polymer concentrations.

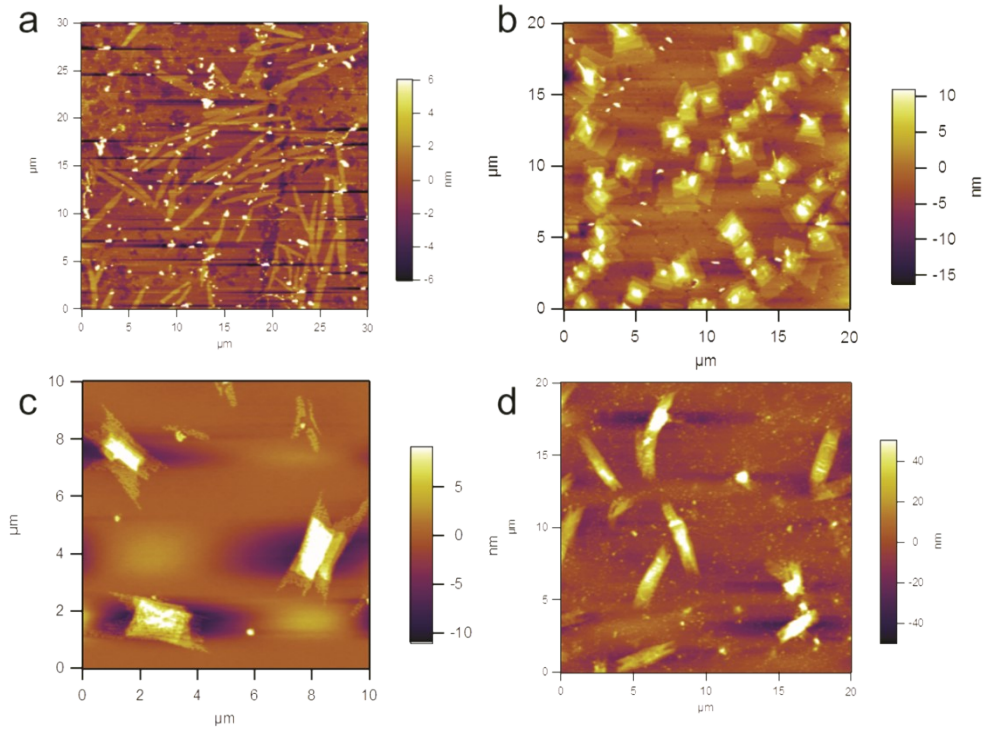

Fig. S9 AFM images of 2D nanostructures formed by P3HT$_{10}$-*b*-PEG$_{12}$ in *i*-PrOH using different polymer concentrations, a) 0.001 mg mL^{-1}, b) 0.005 mg mL^{-1}, c) 0.015 mg mL^{-1}, d) 0.05 mg mL^{-1}.

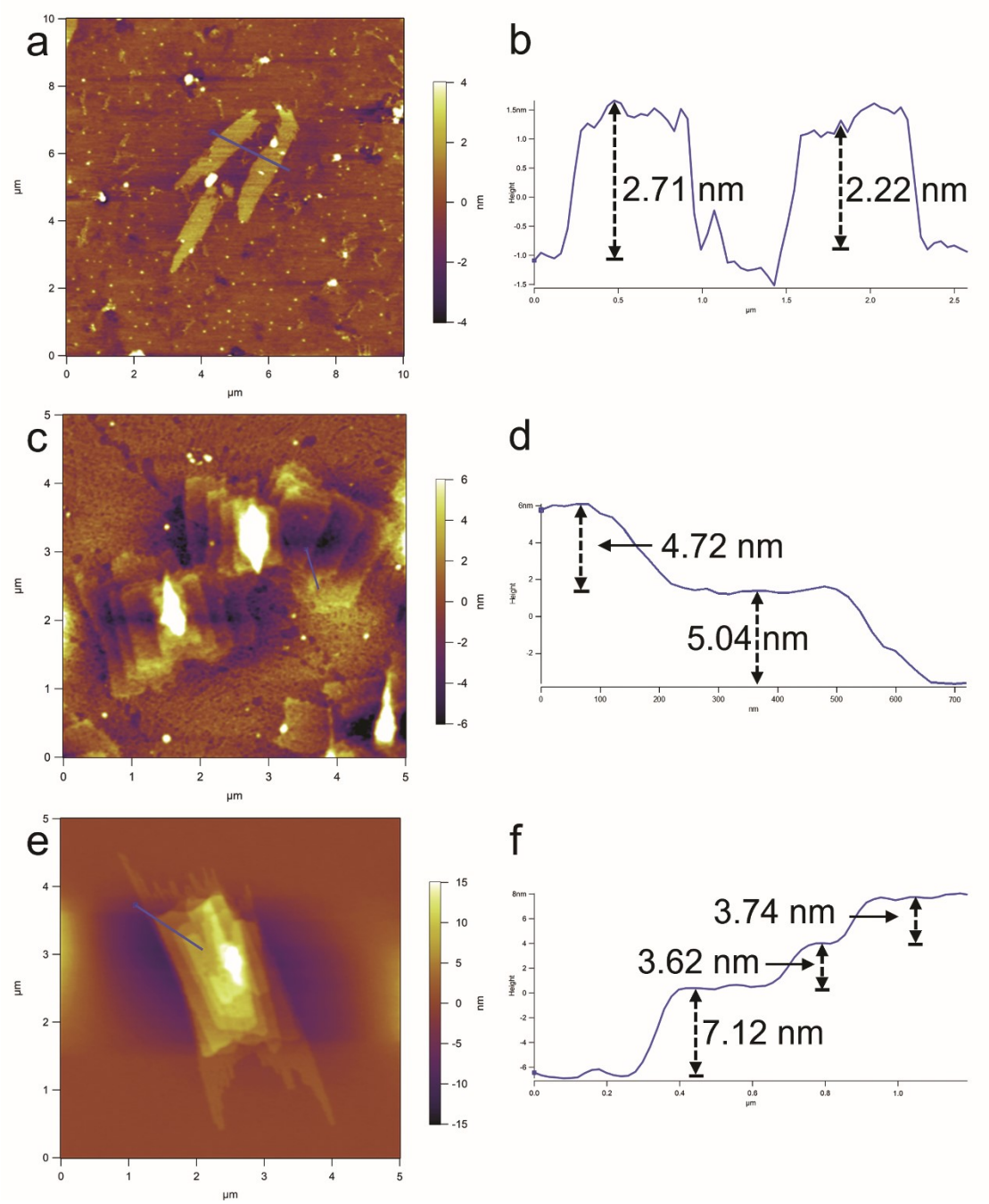

Fig. S10 The AFM images of the 2D micelles and the 2D hierarchical micelles formed by the block copolymer in *i*-PrOH using different polymer concentrations, a, b) 0.001 mg mL^{-1}, c, d) 0.005 mg mL^{-1}, e, f) 0.015 mg mL^{-1}.

10. The estimation of the sizes and conformations of the $P3HT_{10}$ chain.

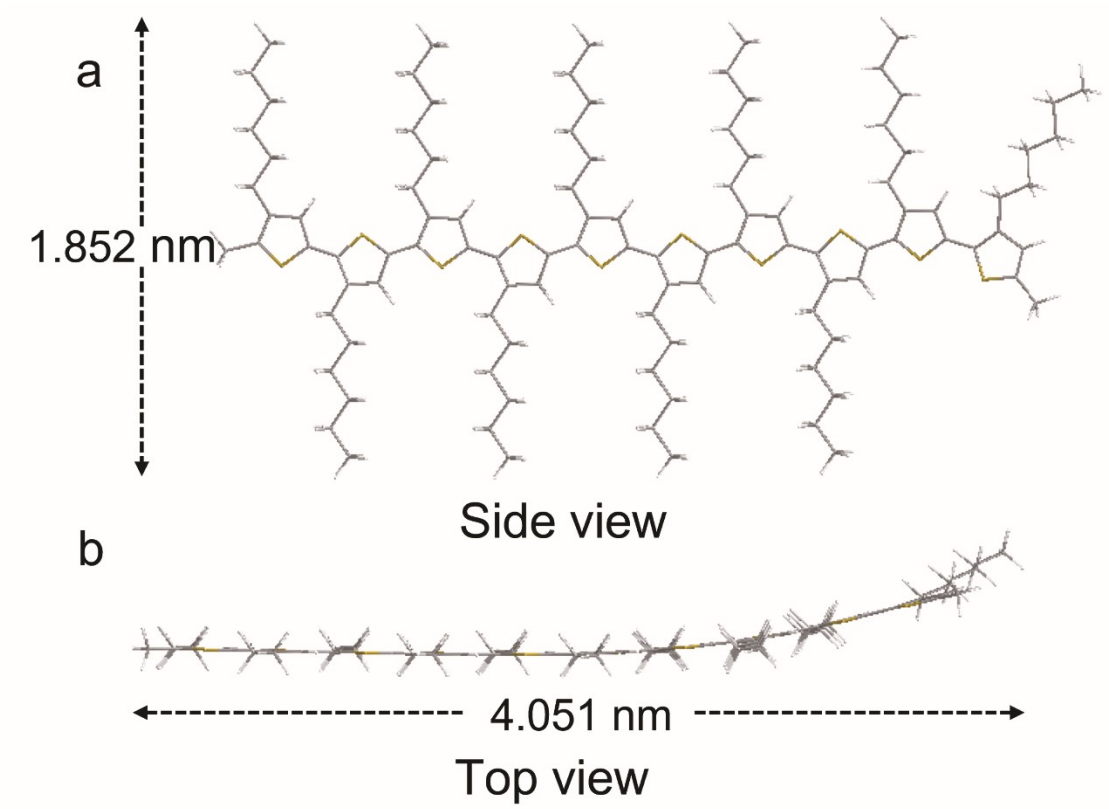

Fig. S11 Top and side views of molecular conformation and the corresponding sizes of the $P3HT_{10}$ chain, calculated with energy minimization (MM2) by ChemBio 3D Ultra, (a) the contour length of the P3HT alkyl chain, (b) the contour length of the conjugated $P3HT_{10}$ backbone.

11. The statistic number of the 2D hierarchical micelles with different laminar layers.

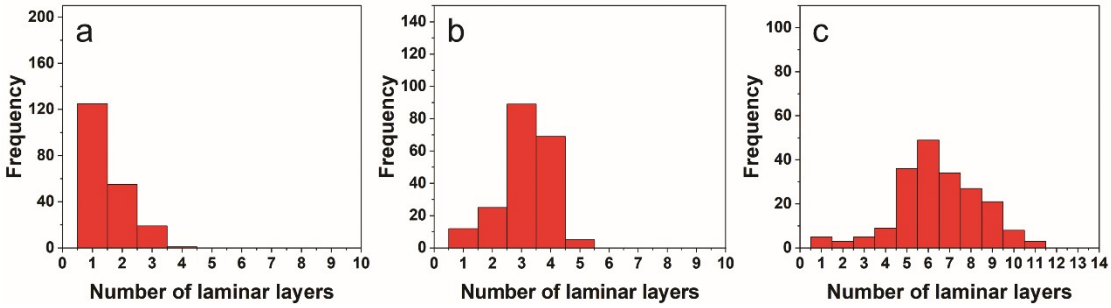

Fig. S12 The statistic number of the 2D hierarchical micelles with different laminar layers formed by P3HT$_{10}$-*b*-PEG$_{12}$ in *i*-PrOH using different polymer concentrations, a) 0.001 mg mL^{-1}, b) 0.005 mg mL^{-1}, c) 0.015 mg mL^{-1}.

12. The HIM images of the 2D hierarchical micelles formed by P3HT$_{10}$-*b*-PEG$_{12}$ in *i*-PrOH (0.015 mg mL^{-1}).

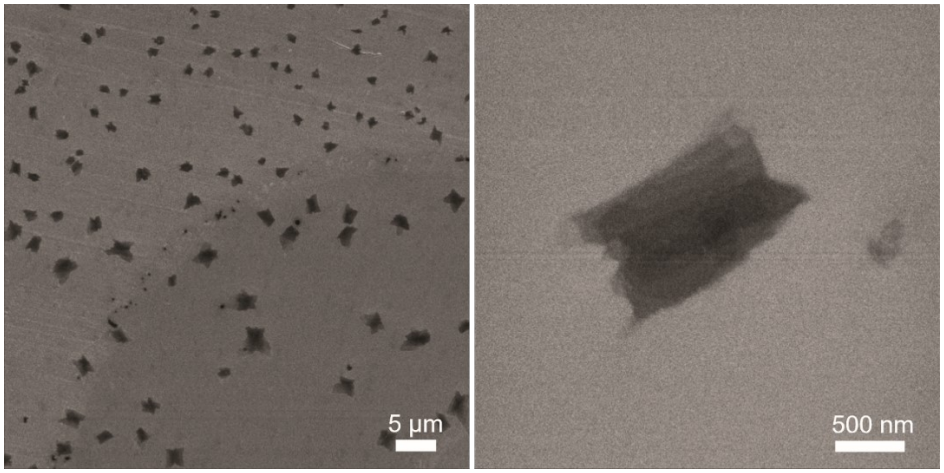

Fig. S13 HIM images of 2D hierarchical micelles formed by P3HT$_{10}$-*b*-PEG$_{12}$ in *i*-PrOH, 0.015 mg mL^{-1}.

13. The probable structure of the ribbon-like P3HT monolayer crystal and the GIWAXS data of the assemblies formed in *i*-PrOH (0.005 mg mL^{-1}).

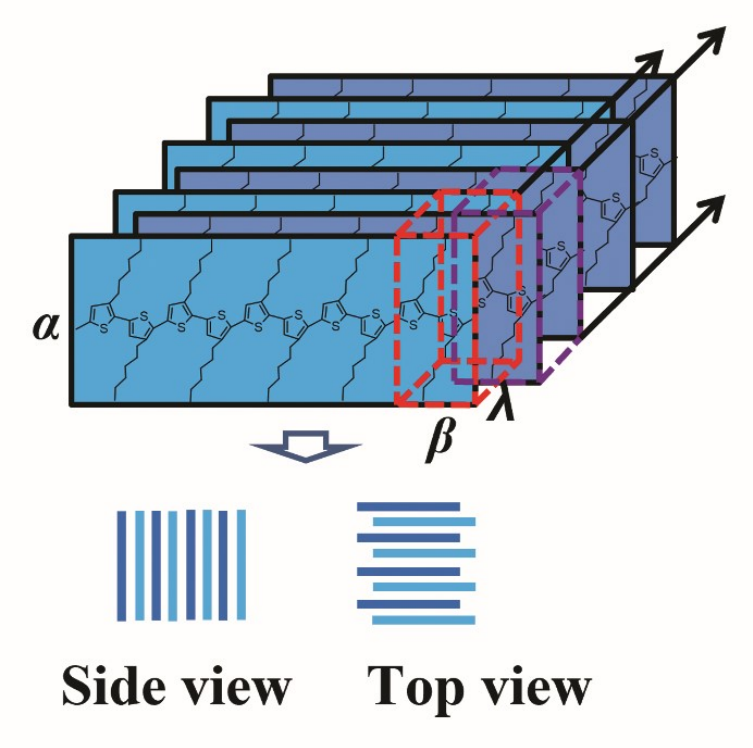

Fig. S14 Probable molecular packing pattern of the ribbon-like P3HT monolayer crystal.

Table S2 Summary of the GIWAXS data.

α (Å)				λ (Å)	
α_1	α_2	α_3	α_4	λ_1	λ_2
11.722	12.200	15.630	16.320	3.657	4.096

14. The TEM images of the nanostructures formed by P3HT$_{10}$-*b*-PEG$_{12}$ (0.005 mg mL^{-1}) in different solutions.

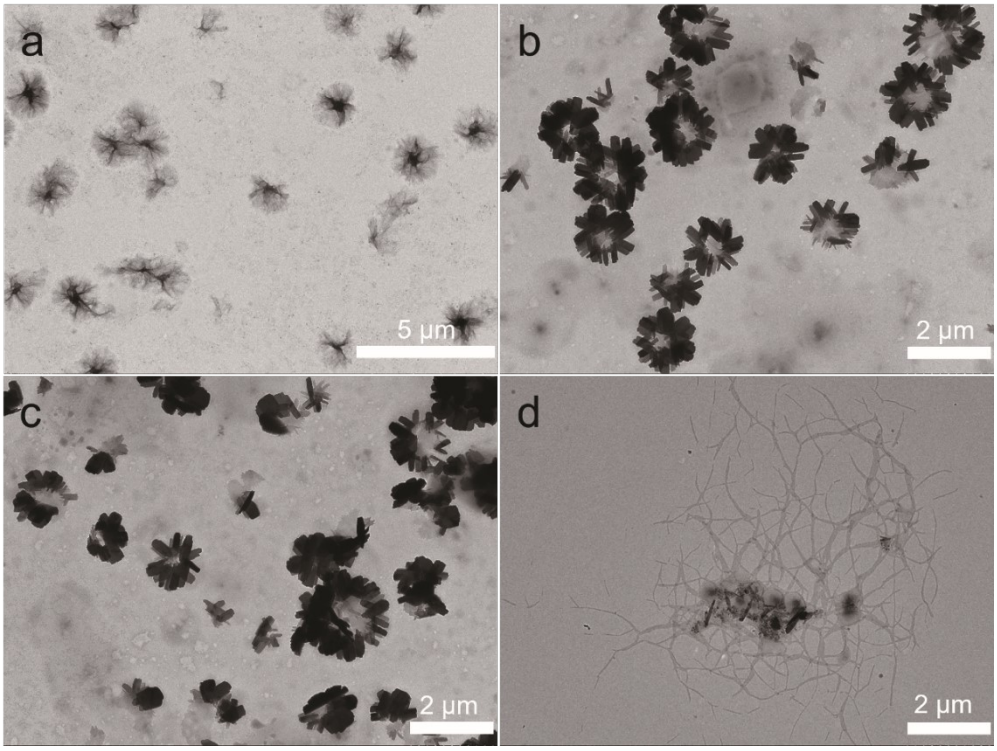

Fig. S15 The TEM images of the nanostructures formed by P3HT$_{10}$-*b*-PEG$_{12}$ (0.005 mg mL^{-1}) in different solutions, a) CH_3OH, b, c) CH_3CH_2OH, d) isobutanol.

15. The size distributions of the 2D nanostructures formed by P3HT$_{10}$-*b*-PEG$_{12}$ in different solutions.

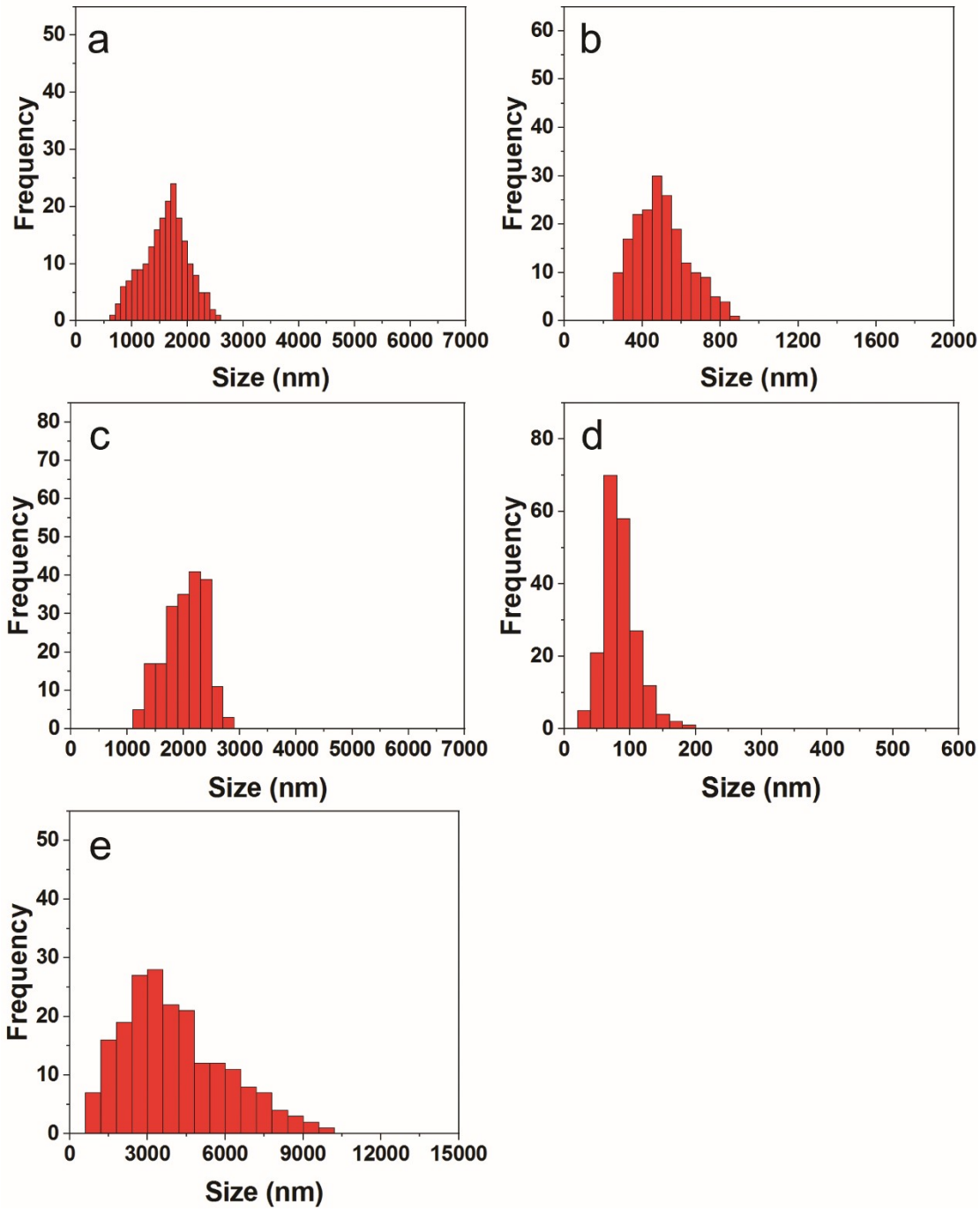

Fig. S16 The diameter distributions of the ball-like micelles (a), the diagonal distributions of 2D micelles (b), the diameter distributions of the flower-like aggregates (c), the width (d) and the contour length distributions (e) of the ribbon-like micelles.

16. The AFM images of the nanostructures formed by $P3HT_{10}$-*b*-PEG_{12} (0.005 mg mL^{-1}) in CH_3CH_2OH and isobutanol.

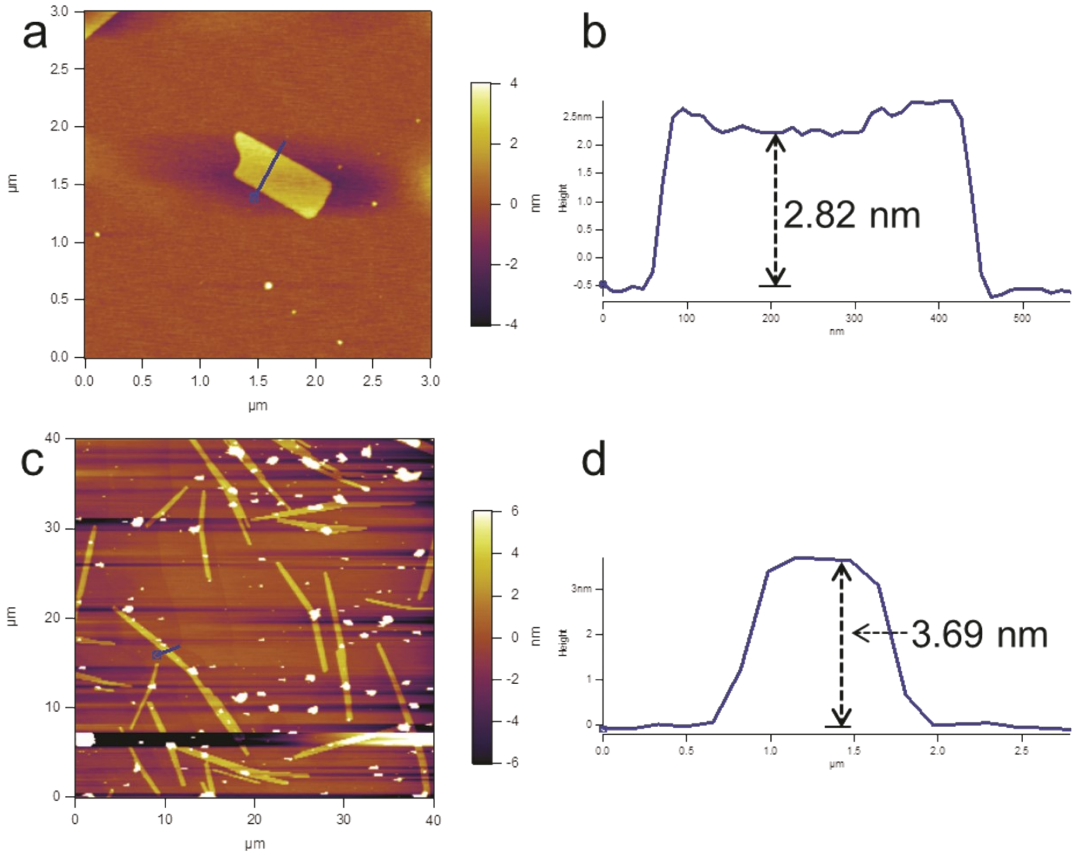

Fig. S17 The AFM images of the nanostructures formed by $P3HT_{10}$-*b*-PEG_{12} (0.005 mg mL^{-1}) in CH_3CH_2OH and isobutanol.

17. The TEM images of the nanostructures formed by $P3HT_{10}$-*b*-PEG_{12} in methanol using different polymer concentrations.

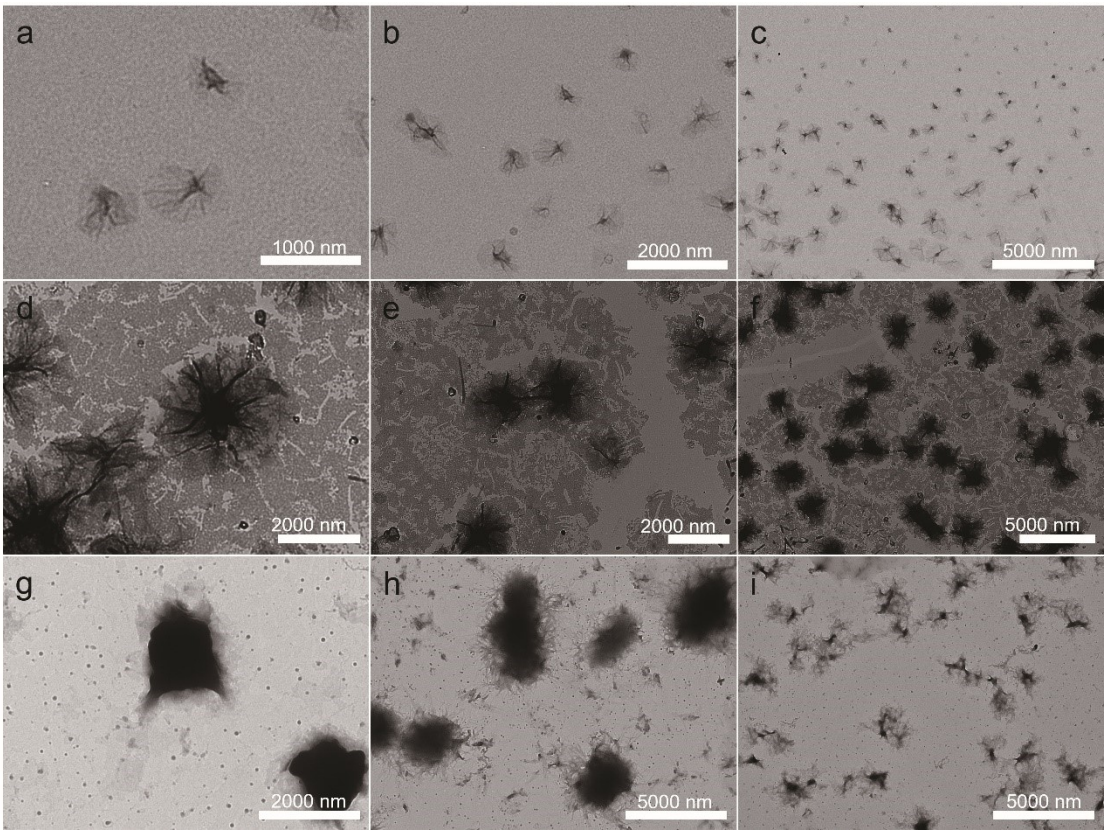

Fig. S18 The TEM images of the nanostructures formed by $P3HT_{10}$-*b*-PEG_{12} in methanol using different polymer concentrations, a, b, c) 0.001 mg mL^{-1}, d, e, f) 0.015 mg mL^{-1}, g, h, i） 0.05 mg mL^{-1}.

18. The size distributions of the nanostructures formed by P3HT$_{10}$-*b*-PEG$_{12}$ in methanol using different polymer concentrations.

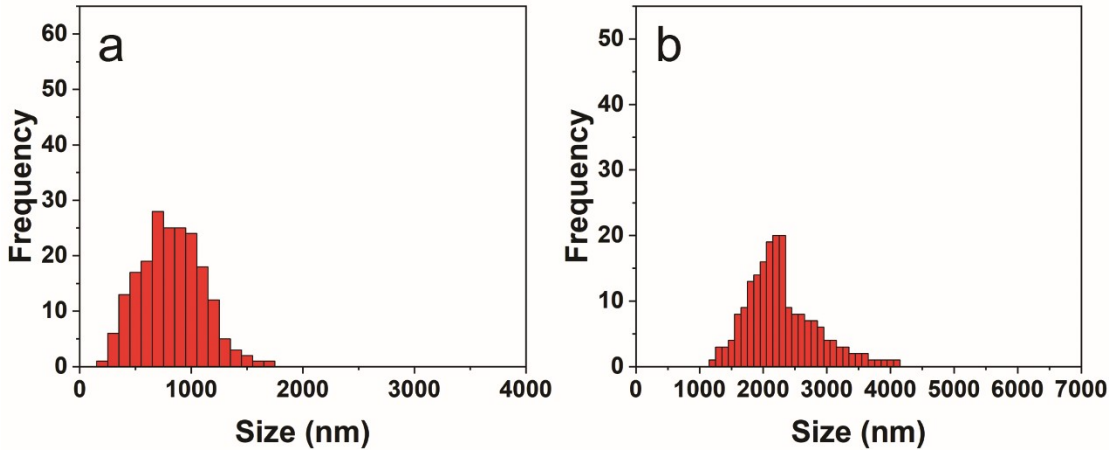

Fig. S19 The diameter distributions of the ball-like nanostructures formed by P3HT$_{10}$-*b*-PEG$_{12}$ in methanol using different polymer concentrations, a) 0.001 mg mL^{-1}, b) 0.015 mg mL^{-1}.

19. The TEM images of the nanostructures formed by P3HT$_{10}$-*b*-PEG$_{12}$ in ethanol using different polymer concentrations.

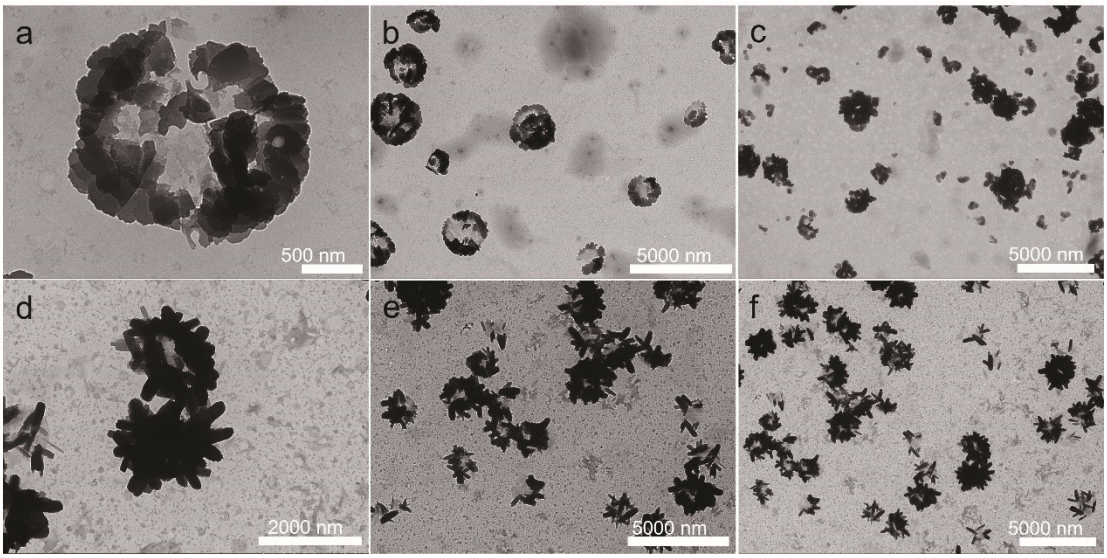

Fig. S20 The TEM images of the nanostructures formed by P3HT$_{10}$-*b*-PEG$_{12}$ in ethanol using different polymer concentrations, a, b, c) 0.001 mg mL^{-1}, d, e, f) 0.05 mg mL^{-1}.

20. The size distributions of the nanostructures formed by P3HT$_{10}$-*b*-PEG$_{12}$ in ethanol using different polymer concentrations.

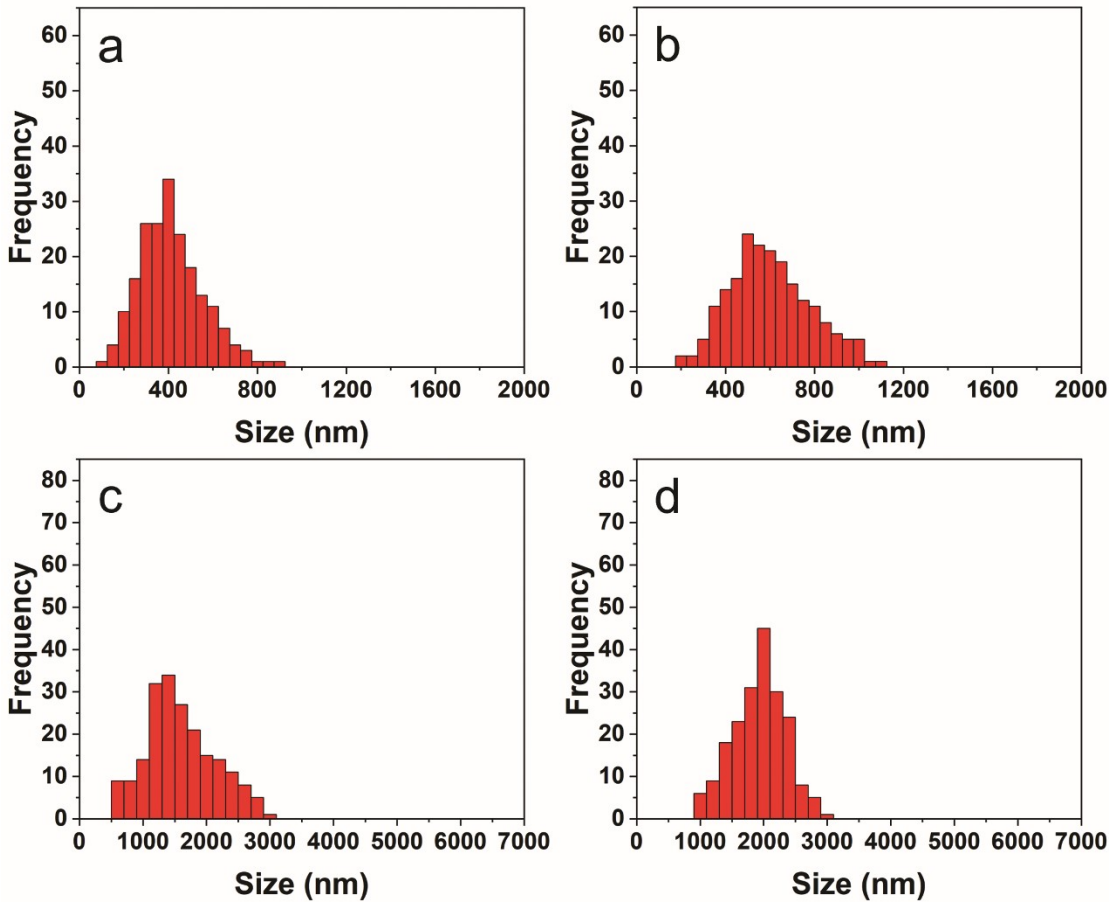

Fig. S21 The diagonal distributions of 2D micelles (a, b), the diameter distributions of the flower-like aggregates (c, d) formed by P3HT$_{10}$-*b*-PEG$_{12}$ in ethanol using different polymer concentrations, a, c) 0.001 mg mL^{-1}, b, d) 0.05 mg mL^{-1}.

21. UV-Vis absorption spectra of P3HT$_{10}$-*b*-PEG$_{12}$ in different solutions.

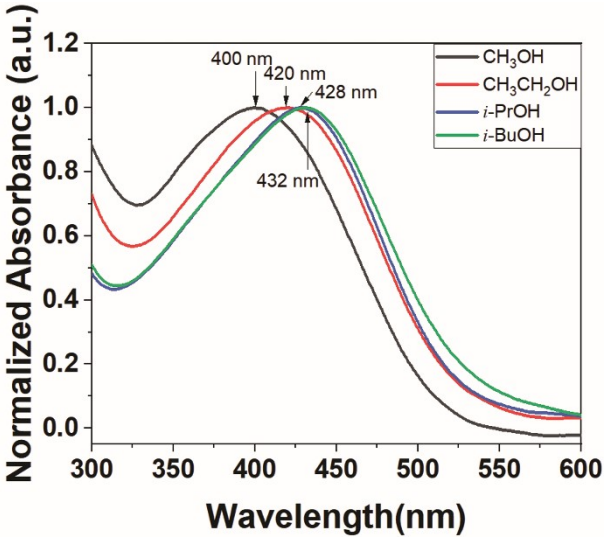

Fig. S22 UV-Vis absorption spectra of P3HT$_{10}$-*b*-PEG$_{12}$ in different solutions (0.005 mg mL^{-1}).

References

1. R. Qi, Y. L. Zhu, L. Han, M. J. Wang and F. He, *Macromolecules*, 2020, **53**, 6555-6565.